

# Magnon Hall Effect without Dzyaloshinskii-Moriya Interaction

S. A. Owerre<sup>1,2</sup>

<sup>1</sup> *Perimeter Institute for Theoretical Physics, 31 Caroline St. N., Waterloo, Ontario N2L 2Y5, Canada.*

<sup>2</sup> *African Institute for Mathematical Sciences, 6 Melrose Road, Muizenberg, Cape Town 7945, South Africa.*

Topological magnon bands and magnon Hall effect in insulating collinear ferromagnets are induced by the Dzyaloshinskii-Moriya interaction (DMI) even at zero magnetic field. In the geometrically frustrated star lattice, a coplanar/noncollinear  $\mathbf{q} = 0$  magnetic ordering may be present due to spin frustration. This magnetic structure, however, does not exhibit topological magnon effects even with DMI in contrast to collinear ferromagnets. We show that a magnetic field applied perpendicular to the star plane induces a non-coplanar spin configuration with nonzero spin scalar chirality, which provides topological effects without the need of DMI. The non-coplanar spin texture originates from the topology of the spin configurations and does not need the presence of DMI or magnetic ordering, which suggests that this phenomenon may be present in the chiral spin liquid phases of frustrated magnetic systems. We propose that these anomalous topological magnon effects can be accessible in Polymeric Iron (III) Acetate — a star-lattice antiferromagnet with both spin frustration and long-range magnetic ordering.

Recently, the experimental observation of thermal Hall effect of spin excitations has been reported in the frustrated Kagomé volborthite  $\text{Cu}_3\text{V}_2\text{O}_7(\text{OH})_2 \cdot 2\text{H}_2\text{O}$  [1] and frustrated honeycomb antiferromagnet  $\text{Ba}_3\text{CuSb}_2\text{O}_9$  [2], with no signs of DMI. This effect has been previously observed in collinear ferromagnetic materials with DMI [3–5] and pyrochlore spin liquid material [6]. In these recent reports, a transverse thermal Hall conductivity  $\kappa_{xy}$  was observed in a strong magnetic field  $\sim 15$  Tesla applied perpendicular to the plane of the frustrated magnets [1, 2]. The observed effect on the Kagomé volborthite is attributed to spin excitations in the spin liquid (SL) regime. However, the Kagomé volborthite is known to exhibit different magnetic-field-induced ordered phases for magnetic fields  $< 15$  Tesla [7, 8]. The frustrated Kagomé compound  $\text{Ca}_{10}\text{Cr}_7\text{O}_{28}$  [9] also exhibits ferromagnetic ordered states for magnetic field of magnitude  $\sim 11$  Tesla. This suggests that the observed low temperature dependence of  $\kappa_{xy}$  in Kagomé volborthite might not be due to spin excitations in the SL regime, but magnon excitations in the field-induced ordered phases. Following these recent developments, we have recently shown [10] that the profile of  $\kappa_{xy}$  in Kagomé volborthite can be captured quantitatively by considering the topological magnon bands in the Kagomé antiferromagnet with/without DMI [11].

The honeycomb-lattice antiferromagnet  $\text{Ba}_3\text{CuSb}_2\text{O}_9$  also shows a negative  $\kappa_{xy}$  at the same magnetic field and a power-law temperature dependence  $\kappa_{xy} \propto T^2$  [2]. It was suggested that the observed thermal Hall effect is a phonon Hall effect. However, a closely related honeycomb-lattice antiferromagnetic material  $\text{Bi}_3\text{Mn}_4\text{O}_{12}(\text{NO}_3)$  [12] shows evidence of magnetic order at a critical field of  $\sim 6$  Tesla consistent with a collinear Néel order [13]. Prior to this experimental report, we have already shown that honeycomb (anti)ferromagnet with a next-nearest-neighbour staggered DMI captures a negative  $\kappa_{xy}$  and power-law temperature dependence  $\kappa_{xy} \propto T^2$  [14, 15] as recently seen in  $\text{Ba}_3\text{CuSb}_2\text{O}_9$  [2]. In this regard, we believe that this correspondence be-

tween theory and experiment cannot be serendipitous. There must be an evidence of field-induced magnetic order in these frustrated antiferromagnetic materials and the associated  $\kappa_{xy}$  must be related to that of magnon excitations.

The star-lattice antiferromagnet is definitely another interesting candidate for realizing nontrivial excitations and thermal Hall conductivity. This lattice can be considered as a variant of the Kagomé lattice by introducing additional lattice links between triangles of the Kagomé lattice. It is also closely related to the honeycomb lattice by shrinking the three-site triangles as one site. However, the star-lattice contains six sites in the unit cell as opposed to the Kagomé and honeycomb lattices. In fact, many different models show interesting features on this lattice [16–23]. A common known material with this lattice structure is Polymeric Iron(III) Acetate,  $\text{Fe}_3(\mu_3\text{-O})(\mu\text{-OAc})_6(\text{H}_2\text{O})_3[\text{Fe}_3(\mu_3\text{-O})(\mu\text{-OAc})_{7.5}]_2 \cdot 7\text{H}_2\text{O}$ , which carries a spin moment of  $S = 5/2$ . In this material, both spin frustration and long-range magnetic ordering coexist at low temperatures [19], but a magnetic field is sufficient to circumvent the spin frustrations and pave the way for long-range magnetic ordering with magnon excitations.

In this Letter, we study the topological properties of geometrically frustrated star lattice antiferromagnet. We focus on the coplanar/noncollinear  $\mathbf{q} = 0$  Néel state, which is definitely a long-range magnetic ordering on the star-lattice induced by spin frustration. In the absence of both the magnetic field and the DMI, there are two flat modes consisting of one zero mode, and four dispersive modes. A nearest-neighbour DMI is known to stabilize the  $\mathbf{q} = 0$  Néel state on the Kagomé lattice [24–30]. This is likely the case on the star lattice. However, in stark contrast to ferromagnets [31–38], the DMI does not lead to topological properties in the  $\mathbf{q} = 0$  Néel state. Hence, the magnon bands remain gapless, leading to vanishing  $\kappa_{xy}$  and no protected chiral edge states. In the presence of an out-of-plane magnetic field, the coplanar  $\mathbf{q} = 0$  Néel state becomes a non-collinear/non-coplanar spin texture. We show that topological ef-

fects are induced by the magnetic field via an induced chiral interaction  $H_\chi \sim \cos \chi \sum \mathbf{S}_i \cdot (\mathbf{S}_j \times \mathbf{S}_k)$ , where  $\cos \chi \propto$  magnetic field. The resulting magnon bands are gapped. We observe a finite  $\kappa_{xy}$  and protected magnon edge states, which persist for zero DMI [39]. It is important to note that the spin scalar chirality survives even in the absence of magnetic ordering  $\langle \mathbf{S}_j \rangle = 0$ , therefore topological effects may be present in chiral spin liquid phase of the star lattice. The proposed phenomenon is very likely to occur in Polymeric Iron(III) Acetate [19].

The model Hamiltonian for our study is given by

$$H = \sum_{\langle i,j \rangle} J_{ij} \mathbf{S}_i \cdot \mathbf{S}_j + \sum_{\langle i,j \rangle} \mathbf{D}_{ij} \cdot \mathbf{S}_i \times \mathbf{S}_j - h \hat{\mathbf{z}} \cdot \sum_i \mathbf{S}_i, \quad (1)$$

where  $J_{ij} = J, J' > 0$  are isotropic antiferromagnetic couplings within and between triangles as shown in Fig. 1.  $\mathbf{D}_{ij}$  is the DMI between sites  $i$  and  $j$  within triangles, and  $h$  is the magnitude of the out-of-plane magnetic field in units of  $g\mu_B$ . On the Kagomé lattice, the  $\mathbf{q} = 0$  ground state is known to be stabilized by an antiferromagnetic next-nearest-neighbour exchange [40] or an out-of-plane DMI,  $\mathbf{D}_{ij} = (0, 0, \mp D_z)$  [24], where  $\mp$  alternates between down and up pointing triangles respectively. Although the DMI alternates between the triangles, only one ground state is selected for each sign with  $D_z > 0$  (positive chirality) and  $D_z < 0$  (negative chirality). In principle a DMI is present on the star-lattice since the midpoint between the bonds connecting two sites is not a center of inversion similar to the Kagomé lattice. Hence, we will assume that the out-of-plane DMI stabilizes the  $\mathbf{q} = 0$  ground state on the star-lattice. It is important to note that the  $\mathbf{q} = 0$  ground state can equally be stabilized through other anisotropy interactions [25]. In most materials, an in-plane DMI may be present, however this component does not induce any topological magnon bands (see Ref. [25]) and it is usually small and can be neglected for simplicity as it does not change any results of this Letter.

In the classical limit, the spin operators can be approximated as classical vectors, written as  $\mathbf{S}_i = S \mathbf{n}_i$ , where  $\mathbf{n}_i = (\sin \chi \cos \theta_i, \sin \chi \sin \theta_i, \cos \chi)$  is a unit vector and  $\theta_i$  labels the spin oriented angles on each sublattice and  $\chi$  is the field-induced canting angle. For the  $\mathbf{q} = 0$  Néel order in Fig. 1,  $\theta_1 = 5\pi/3, \theta_2 = \pi/3, \theta_3 = \pi, \theta_4 = 2\pi/3, \theta_5 = 4\pi/3, \theta_6 = 0$ . The classical energy is given by

$$e_0 = -\frac{J}{2} (1 - 3 \cos^2 \chi) - \frac{J'}{2} (1 - 2 \cos^2 \chi) - \frac{\sqrt{3}}{2} D_z \sin^2 \chi - h \cos \chi, \quad (2)$$

where  $e_0 = E_{cl}/6NS^2$  and the magnetic field is rescaled in unit of  $S$ . Minimizing this energy yields the canting angle  $\cos \chi = h/h_s$ , where  $h_s = (3J + 2J' + \sqrt{3}D_z)$  is the saturation field. For the excitations above the classical ground state, the general procedure is as follows. At zero field, the spins lie on the plane of the star lattice taken

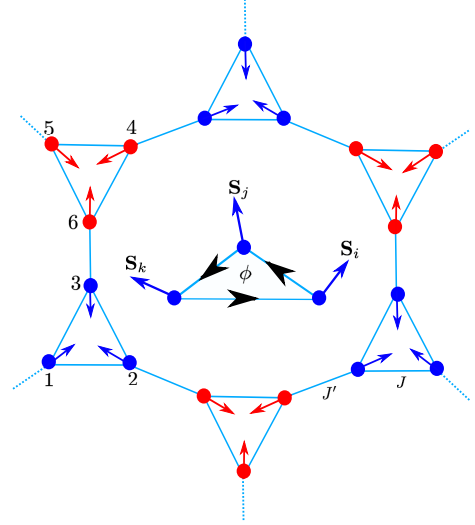


FIG. 1: Color online. The zero field coplanar  $\mathbf{q} = 0$  Néel order on the geometrically frustrated star-lattice. The numbers denote different sublattices. Inset: A nonzero out-of-plane magnetic field generates a non-coplanar spin texture with field-induced fictitious flux ( $\phi$ ) within each triangular plaquette. In Polymeric Iron(III) Acetate [19]  $J' > J$ , hence  $J'/J > 1$ .

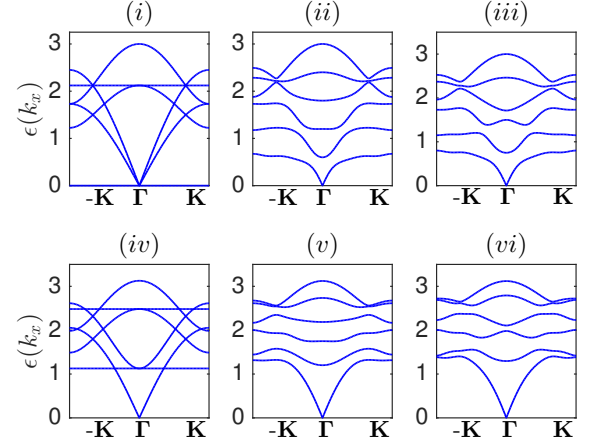


FIG. 2: Color online. Magnon band structure along  $k_y = 0$  with  $J'/J = 1.5$ . For the upper panel  $D_z/J = 0$ : (i)  $h = 0$ , (ii)  $h/h_s = 0.2$ , (iii)  $h/h_s = 0.25$ . For the lower panel  $D_z/J = 0.15$ : (iv)  $h = 0$ , (v)  $h/h_s = 0.2$ , (vi)  $h/h_s = 0.25$ . The linear gapless dispersion of the lowest band at  $\Gamma = (0, 0)$  signifies antiferromagnetic order.

as the  $x$ - $y$  plane as shown in Fig. 1. Then, we perform a rotation about the  $z$ -axis on the sublattices by the spin oriented angles in order to achieve the  $120^\circ$  coplanar Néel order. At this point the quantization axis can be chosen as the  $y$ -axis. As the out-of-plane magnetic field is turned on, the spins cant towards the direction of the field and form a non-coplanar configuration (see inset of Fig. 1). Thus, we have to align them along the new quantization

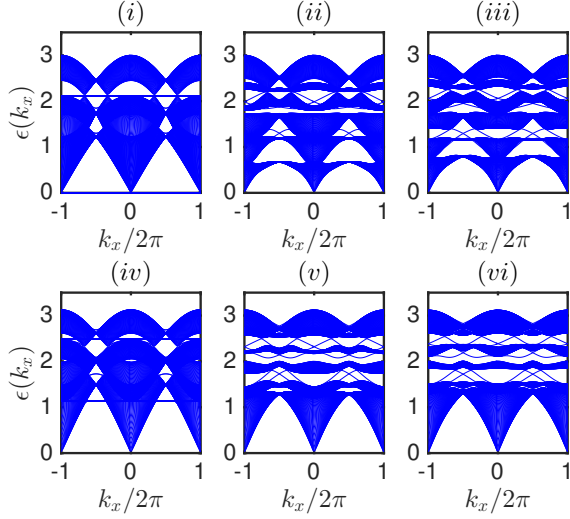


FIG. 3: Color online. The corresponding magnon edge states of Fig. 2 for a strip geometry.

axis by performing a rotation about the  $y$ -axis by the field canting angle  $\chi$ . Hence,

$$\mathbf{S}_i = \mathcal{R}_z(\theta_i) \cdot \mathcal{R}_y(\chi) \cdot \mathbf{S}'_i, \quad (3)$$

where

$$\mathcal{R}_z(\theta_i) \cdot \mathcal{R}_y(\chi) = \begin{pmatrix} \cos \theta_i \cos \chi & -\sin \theta_i & \cos \theta_i \sin \chi \\ \sin \theta_i \cos \chi & \cos \theta_i & \sin \theta_i \sin \chi \\ -\sin \chi & 0 & \cos \chi \end{pmatrix}. \quad (4)$$

We consider the positive chirality ground states,  $\mathbf{D}_{ij} = (0, 0, -D_z)$  with  $D_z > 0$ . The corresponding Hamiltonian that contribute to noninteracting magnon model is given by

$$H_J = J \sum_{\langle i,j \rangle} \left[ \cos \theta_{ij} \mathbf{S}'_i \cdot \mathbf{S}'_j + \sin \theta_{ij} \cos \chi \hat{\mathbf{z}} \cdot (\mathbf{S}'_i \times \mathbf{S}'_j) \right] \quad (5)$$

$$+ 2 \sin^2 \left( \frac{\theta_{ij}}{2} \right) [\sin^2 \chi S_i'^x S_j'^x + \cos^2 \chi S_i'^z S_j'^z],$$

$$H_{J'} = J' \sum_{\langle i,j \rangle} \left[ \cos \theta_{ij} \mathbf{S}'_i \cdot \mathbf{S}'_j + \sin \theta_{ij} \cos \chi \hat{\mathbf{z}} \cdot (\mathbf{S}'_i \times \mathbf{S}'_j) \right] \quad (6)$$

$$+ 2 \sin^2 \left( \frac{\theta_{ij}}{2} \right) [\sin^2 \chi S_i'^x S_j'^x + \cos^2 \chi S_i'^z S_j'^z],$$

$$H_{DMI} = D_z \sum_{\langle i,j \rangle} \left[ \sin \theta_{ij} [\cos^2 \chi S_i'^x S_j'^x + S_i'^y S_j'^y] \right. \quad (7)$$

$$\left. + \sin^2 \chi S_i'^z S_j'^z - \cos \theta_{ij} \cos \chi \hat{\mathbf{z}} \cdot (\mathbf{S}'_i \times \mathbf{S}'_j) \right],$$

$$H_z = -h \cos \chi \sum_i S_i'^z, \quad (8)$$

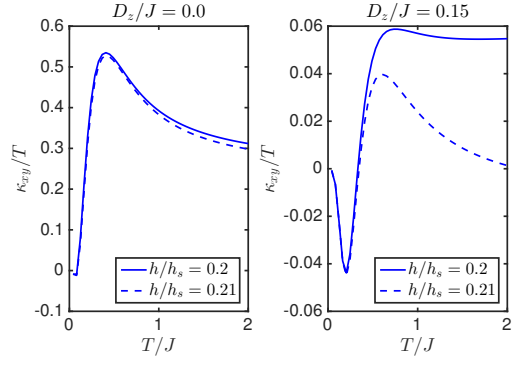


FIG. 4: Color online. Low-temperature dependence of  $\kappa_{xy}$  for two separate DMI and field values at  $J'/J = 1.5$ .

where  $\theta_{ij} = \theta_i - \theta_j$ . The spin scalar chirality  $\mathbf{S}'_k \cdot (\mathbf{S}'_i \times \mathbf{S}'_j)$  with  $\mathbf{S}'_k = \hat{\mathbf{z}}$  is generated by the magnetic field applied perpendicular to the star plane as depicted in the inset of Fig. 1. Evidently, the scalar chirality survives at  $D_z = 0$ , therefore the presence of the DMI is not necessarily needed provided the  $\mathbf{q} = 0$  ordering is stabilized [39]. As mentioned previously, spin scalar chirality is nonzero even when there is no magnetic ordering  $\langle \mathbf{S}_j \rangle = 0$  and can be used as the order parameter in geometrically frustrated systems such as chiral spin liquid states. Therefore, it is possible that the basic result of this Letter can be observed in systems without magnetic ordering but exhibits non-coplanar spin configuration. This is the major difference between the present model and previously studied collinear ferromagnets [31–38].

Interestingly, the coefficient of the chiral interaction  $H_\chi$  vanishes for the  $J'$  coupling between triangles since  $\sin \theta_{ij} = 0$  in the  $J'$  term. This is consistent with the triangular geometry of the star-lattice. Now, we express the spin operators in terms of the Holstein-Primakoff spin boson operators [41]  $S_i'^x = \sqrt{S/2}(b_{i\mu}^\dagger + b_{i\mu})$ ,  $S_i'^y = i\sqrt{S/2}(b_{i\mu}^\dagger - b_{i\mu})$  and  $S_i'^z = S - b_{i,\mu}^\dagger b_{i,\mu}$ . In momentum space the Hamiltonian can be written as

$$H = \frac{S}{2} \sum_{\mathbf{k}} \psi_{\mathbf{k}}^\dagger \cdot \mathcal{H}(\mathbf{k}) \cdot \psi_{\mathbf{k}}, \quad (9)$$

with  $\psi_{\mathbf{k}}^\dagger = (b_{\mu,\mathbf{k}}^\dagger, b_{\mu',\mathbf{k}}^\dagger, b_{\mu,-\mathbf{k}}, b_{\mu',-\mathbf{k}})$ , where  $\mu = 1, 2, 3$  and  $\mu' = 4, 5, 6$ . The Bogoliubov Hamiltonian  $\mathcal{H}(\mathbf{k})$  is a  $12 \times 12$  matrix given by

$$\mathcal{H}(\mathbf{k}) = \begin{pmatrix} \mathbf{A}(\mathbf{k}, \phi) & \mathbf{B}(\mathbf{k}) \\ \mathbf{B}^*(-\mathbf{k}) & \mathbf{A}^*(-\mathbf{k}, \phi) \end{pmatrix}, \quad (10)$$

where

$$\mathbf{A}(\mathbf{k}) = \begin{pmatrix} \mathbf{a}_1(\phi) & \mathbf{b}_1(\mathbf{k}) \\ \mathbf{b}_1(-\mathbf{k}) & \mathbf{a}_1(\phi) \end{pmatrix}, \quad \mathbf{B}(\mathbf{k}) = \begin{pmatrix} \mathbf{a}_2 & \mathbf{b}_2(\mathbf{k}) \\ \mathbf{b}_2(-\mathbf{k}) & \mathbf{a}_2 \end{pmatrix}, \quad (11)$$

$$\mathbf{a}_1(\phi) = \begin{pmatrix} \Delta_0 & \Delta e^{-i\phi} & \Delta e^{i\phi} \\ \Delta e^{i\phi} & \Delta_0 & \Delta e^{-i\phi} \\ \Delta e^{-i\phi} & \Delta e^{i\phi} & \Delta_0 \end{pmatrix}, \quad \mathbf{a}_2 = \Delta' \begin{pmatrix} 0 & 1 & 1 \\ 1 & 0 & 1 \\ 1 & 1 & 0 \end{pmatrix} \quad (12)$$

$$\mathbf{b}_1(\mathbf{k}) = \Lambda \begin{pmatrix} e^{ik_2} & 0 & 0 \\ 0 & e^{ik_1} & 0 \\ 0 & 0 & 1 \end{pmatrix}, \quad \mathbf{b}_2(\mathbf{k}) = \Lambda' \begin{pmatrix} e^{ik_2} & 0 & 0 \\ 0 & e^{ik_1} & 0 \\ 0 & 0 & 1 \end{pmatrix}, \quad (13)$$

where  $\Delta_0 = h_\chi - (\Delta_z + \Lambda_z) = J + J' + \sqrt{3}D_z$ ,  $k_1 = \mathbf{k} \cdot \mathbf{e}_1$  and  $k_2 = \mathbf{k} \cdot \mathbf{e}_2$ . The lattice basis vectors are chosen as  $\mathbf{e}_1 = 2\hat{\mathbf{x}}$  and  $\mathbf{e}_2 = \hat{\mathbf{x}} + \sqrt{3}\hat{\mathbf{y}}$ . The coefficients are given by

$$\Delta_z = 2 \left[ J \left( -\frac{1}{2} + \frac{3}{2} \cos^2 \chi \right) - \frac{\sqrt{3}D_z}{2} \sin^2 \chi \right] \quad (14)$$

$$\Delta = \sqrt{(\Delta_R)^2 + (\Delta_M)^2}, \quad (15)$$

$$\Delta_R = J \left( -\frac{1}{2} + \frac{3 \sin^2 \chi}{4} \right) - \frac{\sqrt{3}D_z}{2} \left( 1 - \frac{\sin^2 \chi}{2} \right), \quad (16)$$

$$\Delta_M = \cos \chi \left( -\frac{\sqrt{3}J}{2} + \frac{D_z}{2} \right), \quad (17)$$

$$\Delta' = \frac{\sin^2 \chi}{2} \left( \frac{3J}{2} + \frac{\sqrt{3}D_z}{2} \right), \quad (18)$$

$$\Lambda_z = J' (-1 + 2 \cos^2 \chi), \quad \Lambda = J' (-1 + \sin^2 \chi), \quad (19)$$

$$\Lambda' = J' \sin^2 \chi, \quad h_\chi = h \cos \chi, \quad (20)$$

and  $\tan \phi_{ij} = \Delta_M / \Delta_R$ . Notice that the fictitious magnetic flux does not vanish at zero DMI unlike in ferromagnets.

In Polymeric Iron(III) Acetate [19], the intra-layer coupling  $J$  is weaker than the inter-layer coupling  $J'$ , hence  $J'/J > 1$ . We have shown the magnon bands in Fig. 2 for  $J'/J = 1.5$ :  $D_z/J = 0$  (upper panel) and  $D_z/J = 0.15$  (lower panel) with several values of the magnetic field  $h/h_s$  along the Brillouin zone (BZ) line  $\pm \mathbf{K} = (\pm 2\pi/3, 0)$ . For  $D_z/J = 0$ , the system exhibits two flat modes and four dispersive bands at  $h/h_s = 0$ . The flat modes contain one zero mode due to the geometry of the star-lattice, and the magnon bands are completely gapless at various points in the BZ. At zero DMI  $D_z/J = 0$ , a moderate increase in the magnetic field lifts the flat zero mode and induces gaps at various points in the magnon bands. Notice that the flat modes also acquire a small dispersion.

For  $D_z/J = 0.15$  the zero mode is lifted at  $h/h_s = 0$ , but the magnon bands remain gapless. As mentioned above, this is due to the fact that the presence of the DMI does not have any topological effects on the  $\mathbf{q} = 0$  Néel state. In fact, this is the major difference between the present model and previously studied collinear ferromagnets [31–38]. As the magnetic field increases from zero the flat modes acquire a small dispersion and the

magnon bands also acquire a gap similar to the case without DMI. The linear gapless dispersion of the lowest band at  $\Gamma$  signifies antiferromagnetic order.

In order to substantiate the nontrivial topology of this system at finite magnetic field, we have solved for the magnon edge states for a strip geometry on the star-lattice as shown in Fig. 3. For zero magnetic field, there is no counter-propagating gapless edge states and the Chern number is zero for all bands, confirming the fact that the system is topologically trivial at zero field. In contrast, for finite magnetic field counter-propagating gapless edge states are discernible in Fig. 3 with a Chern number of  $\pm 1$  signifying the strong topology of the system for nonzero magnetic field irrespective of the DMI. Furthermore, we have confirmed the strong topology of this system at finite field by computing the transverse thermal Hall conductivity  $\kappa_{xy}$  [32, 34]. Figure 4 shows the low-temperature dependence of  $\kappa_{xy}$  for  $D_z/J = 0$  and  $D_z/J = 0.15$  with several field values. As expected,  $\kappa_{xy}$  vanishes at zero magnetic field, and a non-vanishing  $\kappa_{xy}$  is present at finite magnetic field and persists for zero DMI [39].

In summary, the results of this Letter is not simply a consequence of time-reversal symmetry (TRS) breaking, because the magnetic order that underlies magnons has already broken TRS even in ferromagnets. Nevertheless, topological effects do not emerge in the conventional magnonic systems even though TRS is already broken. Another feature of this model is that the magnon bands are not doubly degenerate at zero field as one would expect in TRS invariant systems. This is because magnons are bosonic quasiparticles and the TR operator is defined as  $\mathcal{T}^2 = +1$ , which does not obey Kramers theorem. In this model the broken inversion symmetry of the lattice allows a DMI, but its role is different from ferromagnets, since the coplanar/noncoplanar  $\mathbf{q} = 0$  spin configuration is a consequence of geometric frustration. The basic result of this Letter is that this magnetic ordering is not topological and we showed that topological effects require a topological non-coplanar spin texture with a finite spin scalar chirality. This result originates from the topology of the spin configuration without the need of DMI. It also means that any spin configuration with a non-coplanar structure will exhibit the same effect even when they are not necessarily ordered. Topological Hall effect in non-coplanar systems has been observed in various frustrated electron systems [42–45]. The present model is a magnonic system and we believe that these results can be accessible experimentally in the present and upcoming star-lattice quantum magnetic materials, and can be probed by using neutron inelastic scattering. The magnon edge modes can be probed by edge sensitive methods such as light [46] or electronic [47] scattering method. The experimental study of topological magnon bands and edge state modes are the subjects of current interest [48].

Research at Perimeter Institute is supported by the Government of Canada through Industry Canada and by

- 
- [1] D. Watanabe, K. Sugii, M. Shimozaawa, Y. Suzuki, T. Yajima, H. Ishikawa, Z. Hiroi, T. Shibauchi, Y. Matsuda, M. Yamashita, *Proc. Natl. Acad. Sci. USA* **113**, 8653 (2016).
- [2] Kaori Sugii, Masaaki Shimozaawa, Daiki Watanabe, Yoshitaka Suzuki, Mario Halim, Motoi Kimata, Yosuke Matsumoto, Satoru Nakatsuji, Minoru Yamashita, arXiv:1608.07401.
- [3] Y. Onose, T. Ideue, H. Katsura, Y. Shiomi, N. Nagaosa, Y. Tokura, *Science* **329**, 297 (2010).
- [4] T. Ideue, Y. Onose, H. Katsura, Y. Shiomi, S. Ishiwata, N. Nagaosa, and Y. Tokura, *Phys. Rev. B* **85**, 134411 (2012).
- [5] Max Hirschberger, Robin Chisnell, Young S. Lee, and N. P. Ong, *Phys. Rev. Lett.* **115**, 106603 (2015).
- [6] M. Hirschberger, J. W. Krizan, R. J. Cava, and N. P. Ong, *Science* **348**, 106 (2015).
- [7] M. Yoshida, M. Takigawa, H. Yoshida, Y. Okamoto, and Z. Hiroi, *Phys. Rev. Lett.* **103**, 077207 (2009).
- [8] M. Yoshida, M. Takigawa, S. Kramer, S. Mukhopadhyay, M. Horvatic, C. Berthier, H. Yoshida, Y. Okamoto, Z. Hiroi, *J. Phys. Soc. Jpn.* **81**, 024703 (2012).
- [9] C. Balz, B. Lake, J. Reuther, H. Luetkens, R. Schöne-mann, Th. Herrmannsdörfer, Y. Singh, A. T. M. Nazmul Islam, E. M. Wheeler, J. A. Rodriguez-Rivera, T. Guidi, G. G. Simeoni, C. Baine, and H. Ryll, *Nature Phys.* **12**, 942 (2016).
- [10] S. A. Owerre, arXiv:1608.04561 (2016).
- [11] I. Dzyaloshinsky *J. Phys. Chem. Solids* **4**, 241 1958; T. Moriya *Phys. Rev.* **120**, 91 (1960).
- [12] O. Smirnova, M. Azuma, N. Kumada, Y. Kusano, M. Matsuda, Y. Shimakawa, T. Takei, Y. Yonesaki, and N. Kinomura, *J. Am. Chem. Soc.* **131**, 8313 (2009).
- [13] M. Matsuda, M. Azuma, M. Tokunaga, Y. Shimakawa, and N. Kumada, *Phys. Rev. Lett.* **105**, 187201 (2010).
- [14] S. A. Owerre, *J. Appl. Phys.* **120**, 043903 (2016).
- [15] S. A. Owerre, arXiv:1608.00545 (2016).
- [16] H. Yao and S. A. Kivelson, *Phys. Rev. Lett.* **99**, 247203 (2007).
- [17] Heng-Fu Lin, Yao-Hua Chen, Hai-Di Liu, Hong-Shuai Tao, and Wu-Ming Liu, *Phys. Rev. A* **90**, 053627 (2014).
- [18] J. Richter, J. Schulenburg, A. Honecker, and D. Schmal-fuß *Phys. Rev. B* **70**, 174454 (2004).
- [19] Y. -Z. Zheng, M. -L. Tong, W. Xue, W. -X. Zhang, X. -M. Chen, Fe. Grandjean, G. J. Long, *Angew. Chem., Int. Ed.* **46**, 6076 (2007).
- [20] J. O. Fjaerestad, arXiv:0811.3789.
- [21] B.-J. Yang, A. Paramakanti, and Y. B. Kim, *Phys. Rev. B* **81**, 134418 (2010).
- [22] W. -C. Chen, R. Liu, Y. -F. Wang, and C. -D. Gong, *Phys. Rev. B* **86**, 085311 (2012).
- [23] A. Rüegg, J. Wen, and G. A. Fiete, *Phys. Rev. B* **81**, 205115 (2010).
- [24] M. Elhajal, B. Canals, and C. Lacroix, *Phys. Rev. B* **66**, 014422 (2002).
- [25] K. Matan, D. Grohol, D. G. Nocera, T. Yildirim, A. B. Harris, S. H. Lee, S. E. Nagler, and Y. S. Lee, *Phys. Rev. Lett.* **96**, 247201 (2006).
- [26] O. Cépas, C. M. Fong, P. W. Leung, and C. Lhuillier *Phys. Rev. B* **78**, 140405(R) (2008).
- [27] A. Zorko, S. Nellutla, J. van Tol, L. C. Brunel, F. Bert, F. Duc, J.-C. Trombe, M. A. de Vries, A. Harrison, and P. Mendels, *Phys. Rev. Lett.* **101**, 026405 (2008).
- [28] H. Yoshida, Y. Michiue, E. Takayama-Muromachi, and M. Isobe, *J. Mater. Chem.* **22**, 18793 (2012).
- [29] A. Zorko, F. Bert, A. Ozarowski, J. van Tol, D. Boldrin, A. S. Wills, and P. Mendels, *Phys. Rev. B* **88**, 144419 (2013).
- [30] A. L. Chernyshev, *Phys. Rev. B* **92**, 094409 (2015).
- [31] H. Katsura, N. Nagaosa, and P. A. Lee, *Phys. Rev. Lett.* **104**, 066403 (2010).
- [32] R. Matsumoto and S. Murakami, *Phys. Rev. Lett.* **106**, 197202 (2011); *Phys. Rev. B* **84**, 184406 (2011).
- [33] L. Zhang, J. Ren, J. S. Wang, and B. Li, *Phys. Rev. B* **87**, 144101 (2013).
- [34] R. Matsumoto, R. Shindou, and S. Murakami, *Phys. Rev. B* **89**, 054420 (2014).
- [35] H. Lee, J. H. Han, and P. A. Lee, *Phys. Rev. B* **91**, 125413 (2015).
- [36] A. Mook, J. Henk, and I. Mertig, *Phys. Rev. B* **90**, 024412 (2014); A. Mook, J. Henk, and I. Mertig, *Phys. Rev. B* **89**, 134409 (2014).
- [37] S. A. Owerre, *J. Phys.: Condens. Matter* **28**, 386001 (2016).
- [38] A. A. Kovalev and V. Zyuzin, *Phys. Rev. B* **93**, 161106(R) (2016).
- [39] For zero DMI, the coplanar  $\mathbf{q} = 0$  magnetic order can be stabilized by other non-chiral anisotropy interactions such as an easy plane anisotropy. In this case, the magnetic field still induces a non-coplanar spin texture with nonzero spin scalar chirality and a nonzero thermal Hall conductivity as shown in the text.
- [40] A. B. Harris, C. Kallin, and A. J. Berlinsky, *Phys. Rev. B* **45**, 2899 (1992).
- [41] T. Holstein and H. Primakoff, *Phys. Rev.* **58**, 1098 (1940).
- [42] Y. Taguchi, Y. Oohara, H. Yoshizawa, N. Nagaosa, Y. Tokura, *Science* **291**, 2573 (2001).
- [43] Y. Machida, S. Nakatsuji, Y. Maeno, T. Tayama, T. Sakakibara, and S. Onoda, *Phys. Rev. Lett.* **98**, 057203 (2007).
- [44] Y. Machida, S. Nakatsuji, S. Onoda, T. Tayama, and T. Sakakibara, *Nature*, **463**, 210 (2008).
- [45] Jian Zhou, Qi-Feng Liang, Hongming Weng, Y. B. Chen, Shu-Hua Yao, Yan-Feng Chen, Jinming Dong, and Guang-Yu Guo, *Phys. Rev. Lett.* **116**, 256601 (2016).
- [46] Luuk J. P. Ament, Michel van Veenendaal, Thomas P. Devereaux, John P. Hill, and Jeroen van den Brink, *Rev. Mod. Phys.* **83**, 705 (2011).
- [47] Khalil Zakeri, *Physics Reports* **545**, 47 (2014).
- [48] R. Chisnell, J. S. Helton, D. E. Freedman, D. K. Singh, R. I. Bewley, D. G. Nocera, and Y. S. Lee, *Phys. Rev. Lett.* **115**, 147201 (2015).